OXFORD

Human Molecular Genetics, 2023, Vol. 32, 15, 2523–2531
https://doi.org/10.1093/hmg/ddad083
Advance access publication date 23 May 2023
Original Article

Rare protective variants and glaucoma-relevant cell stressors modulate *Angiopoietin-like 7* expression

Inas F. Aboobakar[1], Edward Ryan A. Collantes[1], Michael A. Hauser[2], W. Daniel Stamer[2,3] and Janey L. Wiggs[1,*]

[1]Department of Ophthalmology, Massachusetts Eye and Ear, Harvard Medical School, Boston, MA 02115, USA
[2]Department of Ophthalmology, Duke University School of Medicine, Durham, NC 27710, USA
[3]Department of Biomedical Engineering, Duke University School of Medicine, Durham, NC 27710, USA

*To whom correspondence should be addressed at: Department of Ophthalmology, Massachusetts Eye and Ear, Harvard Medical School, 243 Charles St., Boston, MA 02114, USA. Tel: +617-573-6440; Fax: +617-573-3152; Email: janey_wiggs@meei.harvard.edu

Abstract

Rare missense and nonsense variants in the *Angiopoietin-like 7* (*ANGPTL7*) gene confer protection from primary open-angle glaucoma (POAG), though the functional mechanism remains uncharacterized. Interestingly, a larger variant effect size strongly correlates with *in silico* predictions of increased protein instability ($r = -0.98$), suggesting that protective variants lower *ANGPTL7* protein levels. Here, we show that missense and nonsense variants cause aggregation of mutant *ANGPTL7* protein in the endoplasmic reticulum (ER) and decreased levels of secreted protein in human trabecular meshwork (TM) cells; a lower secreted:intracellular protein ratio strongly correlates with variant effects on intraocular pressure ($r = 0.81$). Importantly, accumulation of mutant protein in the ER does not increase expression of ER stress proteins in TM cells ($P > 0.05$ for all variants tested). Cyclic mechanical stress, a glaucoma-relevant physiologic stressor, also significantly lowers *ANGPTL7* expression in primary cultures of human Schlemm's canal (SC) cells (−2.4-fold-change, $P = 0.01$). Collectively, these data suggest that the protective effects of *ANGPTL7* variants in POAG stem from lower levels of secreted protein, which may modulate responses to physiologic and pathologic ocular cell stressors. Downregulation of *ANGPTL7* expression may therefore serve as a viable preventative and therapeutic strategy for this common, blinding disease.

Introduction

Glaucoma is the leading cause of irreversible blindness worldwide and the prevalence is rising as global populations age (1). Primary open-angle glaucoma (POAG) is the most common subtype, affecting ~68 million individuals (2). Elevated intraocular pressure (IOP), due to dysfunctional aqueous humor outflow, is a strong risk factor and the target of all current POAG therapies. However, these therapies do not target the underlying molecular mechanisms responsible for disease development, which limits their efficacy.

Interestingly, a rare variant analysis performed in the UK Biobank and FinnGen datasets identified four missense and one nonsense variant in the *Angiopoietin-like 7* (*ANGPTL7*) gene that are associated with lower IOP and decreased odds of developing POAG (Table 1) (3). *ANGPTL7* is one of eight angiopoietin-like genes, which have various biological functions relevant to health and disease, including roles in inflammation, angiogenesis and lipid/glucose metabolism (4). *ANGPTL7* is highly expressed in the juxtacanalicular region, which is the site of greatest resistance in the aqueous outflow pathway (5–7). Moreover, *ANGPTL7* expression is higher in POAG patients compared with controls (6); is increased in response to disease-relevant pathologic stressors (dexamethasone and TGF-β) (8–10); and leads to altered expression of extracellular matrix (ECM) genes (10). Collectively, these data support a functional role for *ANGPTL7* in POAG pathogenesis and suggest that modulating its expression may be a viable therapeutic strategy.

However, the precise mechanism whereby *ANGPTL7* variants confer disease protection remains uncharacterized. Elucidating this functional mechanism is a crucial first step for harnessing *ANGPTL7* modulation as a novel glaucoma therapy. In this study, we (i) use *in silico* analyses to estimate the effects of protective variants on *ANGPTl7* protein stability; (ii) examine cellular localization and secretion of wild-type (WT) versus variant *ANGPTL7*; (iii) assess the impact of protective variants on endoplasmic reticulum (ER) stress; and (iv) explore whether cyclic mechanical stress (CMS), a key physiologic stressor in the aqueous outflow pathway, alters *ANGPTL7* expression.

Results

Protective *ANGPTL7* variants impact protein stability

All known protective variants in the *ANGPTL7* locus cause missense and nonsense changes in the C-terminal fibrinogen-like domain (Fig. 1A). We hypothesized that these coding variants impact protein folding and stability. To test this hypothesis, we estimated protein stability using FoldX software (11). The target residue for each missense variant was mutated individually and the difference in free energy ($\Delta\Delta G$) relative to WT *ANGPTL7* protein was calculated; the FoldX software does not enable analysis of nonsense mutations so the Arg177Ter mutation could not be assessed.

Of the four missense variants, three had destabilizing effects (Arg140His, Gln175His, Arg220Cys), whereas the fourth variant had a neutral effect (Gln136Arg) (Fig. 1B). We then assessed the correlation between degree of protein instability ($\Delta\Delta G$ value)

Received: March 22, 2023. **Revised:** May 10, 2023. **Accepted:** May 11, 2023

Table 1. Rare protective *ANGPTL7* variants. Minor allele frequencies and effect size estimates (glaucoma OR and effect on IOPcc) were obtained from the UK Biobank/FinnGen rare variant analysis (3)

Variant rsID	Nucleotide change	Amino acid change	Minor allele frequency (UK/Finland)	Glaucoma OR (95% CI)	Effect on IOPcc in mmHg (95% CI)
rs200058074	A/G	Gln136Arg	0.11%/NA	NS	−0.05 (−0.89, 0.79)
rs28991002	G/A	Arg140His	0.51%/0.35%	NS	−0.23 (−0.59, 0.14)
rs28991009	G/T	Gln175His	1.43%/0.24%	0.64 (**) (0.48, 0.87)	−0.53 (***) (−0.73, −0.32)
rs143435072	C/T	Arg177Ter	0.07%/NA	NS	−0.46 (−1.4, 0.5)
rs147660927	C/T	Arg220Cys	NA/7.82%	0.67 (***) (NA)	NA

OR = odds ratio; IOPcc = corneal-compensated intraocular pressure; CI = confidence interval; mmHg = millimeters of mercury; NS = not significant; NA = not available; $^{**}P < 0.01$; $^{***}P < 0.001$

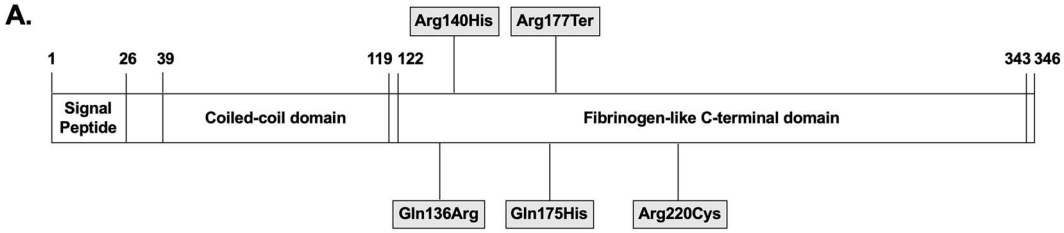

B.

Protective Variant	FoldX ΔΔG (kcal/mol)	Effect on IOPcc in UK Biobank
Gln136Arg	-0.019	-0.05 mmHg
Arg140His	0.722	-0.23 mmHg
Gln175His	2.934	-0.53 mmHg
Arg177Ter	Unable	-0.46 mmHg
Arg220Cys	2.112	N/A

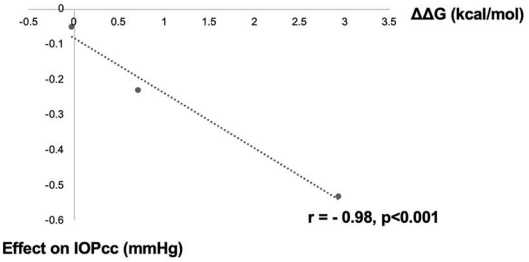

Figure 1. ANGPTL7 protein structure and impact of protective variants on protein stability. (**A**) ANGPTL7 is a secreted protein comprised of an N-terminal coiled-coil domain and a C-terminal fibrinogen-like domain. The amino acid positions corresponding to the protein domains are listed. Interestingly, all five known variants conferring protection from primary open-angle glaucoma are located in the C-terminal fibrinogen-like domain. (**B**) FoldX software was used to estimate the effects of protective *ANGPTL7* variants on protein stability. The target residues for each protective variant were mutated individually and the difference in free energy (ΔΔG) relative to wild-type *ANGPTL7* protein was calculated for each of the mutant proteins. A ΔΔG value >+0.5 indicates a destabilizing effect, whereas a value <−0.5 indicates a stabilizing effect; a value between −0.5 and +0.5 indicates a neutral change. Given the FoldX software does not enable analysis of nonsense mutations, the ΔΔG for the Arg177Ter mutation could not be calculated. The correlation between ΔΔG values and corneal-compensated intraocular pressure (IOPcc) lowering among individuals in the UK Biobank dataset (Table 1) was assessed using Pearson's correlation coefficient (r). There was a strong correlation between greater protein instability and larger effects on IOPcc ($r = -0.98$, $n = 3$, $P < 0.001$), suggesting that protective variants lower Angptl7 expression.

and variant effects on corneal-compensated intraocular pressure (IOPcc) among individuals in the UK Biobank dataset (Table 1) (3). Interestingly, there was a strong correlation between greater protein instability and larger amounts of IOPcc lowering ($r = -0.98$, $n = 3$, $P < 0.001$), suggesting that the protective effects of *ANGPTL7* variants stem from reduced protein levels (Fig. 1B).

Localization of WT and variant *ANGPTL7* protein

Given the predicted effects of protective variants on protein stability, we assessed their impact on cellular localization of *ANGPTL7* protein using immunohistochemistry. COS-7 (African green monkey kidney fibroblast-like) cells were chosen for this experiment given the relatively large cell size compared with HEK293 (human embryonic kidney) cells, enabling better image resolution (12). Cells were transfected with an expression vector containing either WT *ANGPTL7* or one of the five protective variants tagged with a V5-epitope (Supplementary Material, Fig. S1). The expression vector also contained a GFP reporter gene under the control of an internal ribosome entry site (IRES). DAPI nuclear staining and ER staining (CellLight™ ER-RFP) were also performed. Minimal cell death was noted post-transfection, with no significant differences noted among the empty vector, WT and variant *ANGPTL7* constructs (data not shown).

WT *ANGPTL7* protein had diffuse cellular localization and, interestingly, the five protective variants had variable effects on localization (Fig. 2). The Gln136Arg and Arg140His variants had diffuse staining pattern similar to WT. In contrast, the Gln175His, Arg177Ter and Arg220Cys variants were largely confined to the ER, with little to no cytoplasmic staining noted. This experiment was subsequently repeated in primary cultures of human trabecular meshwork (TM) cells (two strains from different donors), which demonstrated similar findings (Fig. 2).

Protective variants reduce amounts of secreted *ANGPTL7* protein

Aggregation of variant *ANGPTL7* protein in the ER suggested that these variants impact its secretion. To test this hypothesis, western blot analysis of intracellular (IC) and extracellular (EC) *ANGPTL7* protein levels was performed. HEK293 cells and primary cultures of human TM cells were transfected with either empty vector, WT *ANGPTL7* or one of the five protective variants tagged with a V5-epitope (Supplementary Material, Fig. S1). Each vector was tested in triplicate in HEK293 cells ($n = 3$). Additionally, two

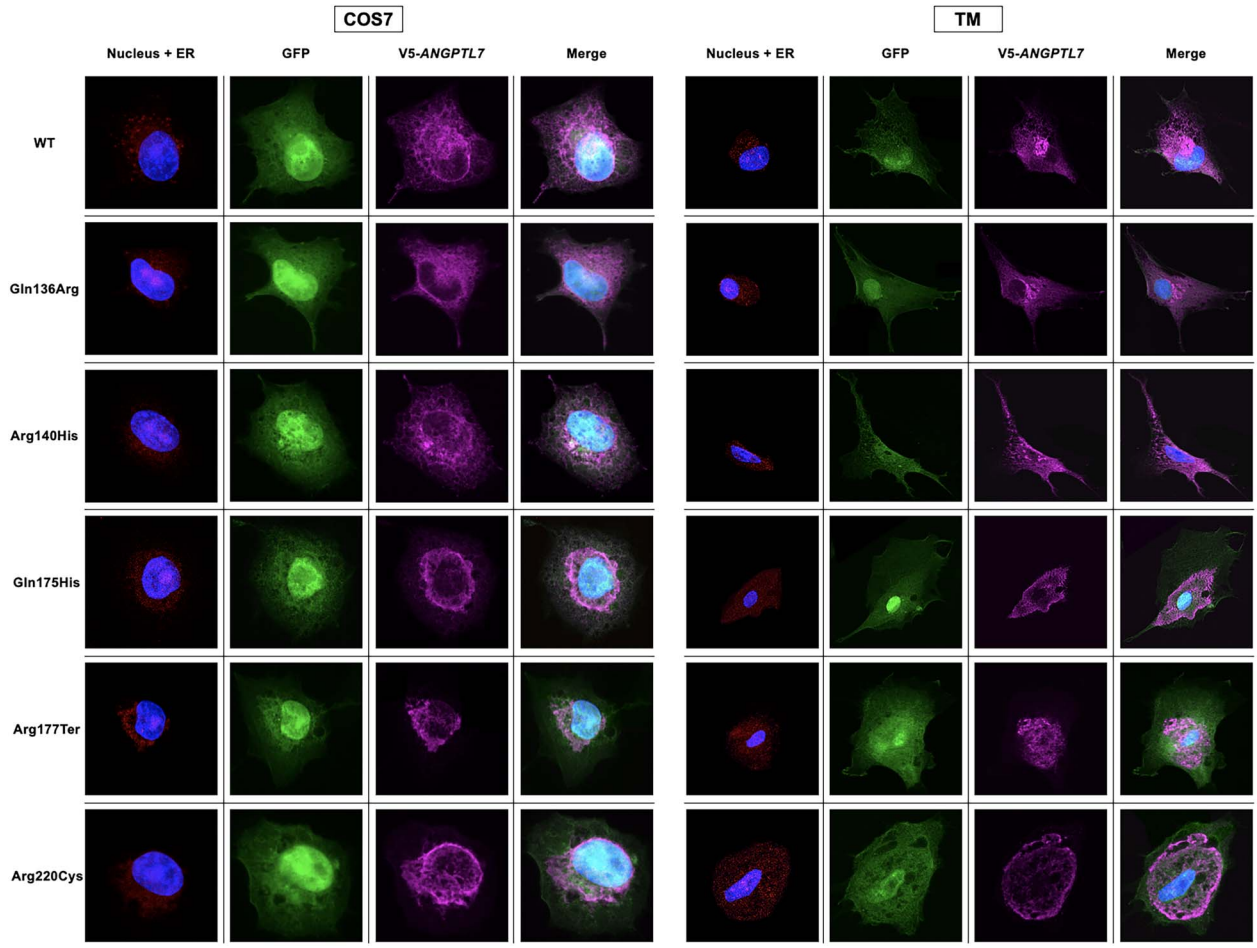

Figure 2. Localization of wild-type and variant *ANGPTL7* in COS-7 and human TM cells**.** Cells were transfected with an expression vector containing either wild-type (WT) *ANGPTL7* or one of the five protective variants tagged with a V5-epitope. The expression vector also contained a GFP reporter gene under the control of an internal ribosome entry site (IRES). In addition, DAPI nuclear staining and endoplasmic reticulum (ER) staining were performed. In both COS-7 and TM cells, WT *ANGPTL7* has diffuse cellular staining; although some variant proteins also have diffuse cellular localization, others are confined to the ER.

TM strains from different donors were each tested in duplicate ($n = 4$). Whole-cell lysates (IC protein) and conditioned media (EC protein) were collected 48-hours post-transfection.

In both HEK293 and TM cells, western blot showed truncated IC *ANGPTL7* protein products for the Arg177Ter nonsense variant, whereas all other variants showed protein products of expected size (~45 kDa with a doublet band due to post-translational glycosylation (10)) (Fig. 3A). Of note, a smaller EC protein product was noted in TM cells compared with HEK293 cells, possibly due to proteolytic cleavage. There was no EC protein detected for the Arg177Ter and Arg220Cys variants in TM cells, whereas the other variants had varying levels of protein secretion. No IC or EC protein was detected with transfection of empty vector alone.

The levels of EC and IC *ANGPTL7* protein were quantified for each variant and normalized relative to WT for both HEK293 and TM cells; a ratio of EC:IC *ANGPTL7* was also calculated (Fig. 3B). The Arg220Cys variant had significantly lower IC levels of *ANGPTL7* protein on western blot compared with WT in both HEK293 and TM cells ($P < 0.05$). EC levels of the Arg177Ter and Arg220Cys variants were also reduced compared with WT in both cell types. Additionally, the ratio of EC:IC protein was reduced for three of the five protective variants in both HEK293 and TM cells [Gln175His ($P < 0.05$), Arg177Ter and Arg220Cys] (*P*-values were not able to be derived for some variants due to zero count) (Fig. 3B).

To confirm that the differences in protein levels were not due to reduced *ANGPTL7* expression, the two TM strains were each transfected with either WT *ANGPTL7* or one of the five protective variants. Quantitative polymerase chain reaction (qPCR) was performed 48 hours post-transfection, which confirmed that the variants did not lead to reduced *ANGPTL7* mRNA levels relative to WT (Supplementary Material, Fig. S2).

These data suggested that the protective effects of *ANGPTL7* variants stem from reduced amounts of secreted protein. To further explore this hypothesis, we assessed the correlation between EC:IC *ANGPTL7* ratios in HEK293 and TM cells and variant effects on corneal-compensated intraocular pressure (IOPcc) among individuals in the UK Biobank dataset (Table 1) (3). Interestingly, there was a strong correlation between lower EC:IC ratio and larger amounts of IOPcc lowering ($r = 0.86$ in HEK293 cells and 0.81 in TM cells), though this did not reach statistical significance due to the small number of data points ($P = 0.14$ for HEK293 cells and 0.19 for TM cells, $n = 4$ for each) (Fig. 3C).

Aggregation of mutant *ANGPTL7* protein in the ER does not increase expression of ER stress markers

Accumulation of mutant proteins in the ER can lead to increased ER stress and cellular cytotoxicity in the conventional aqueous

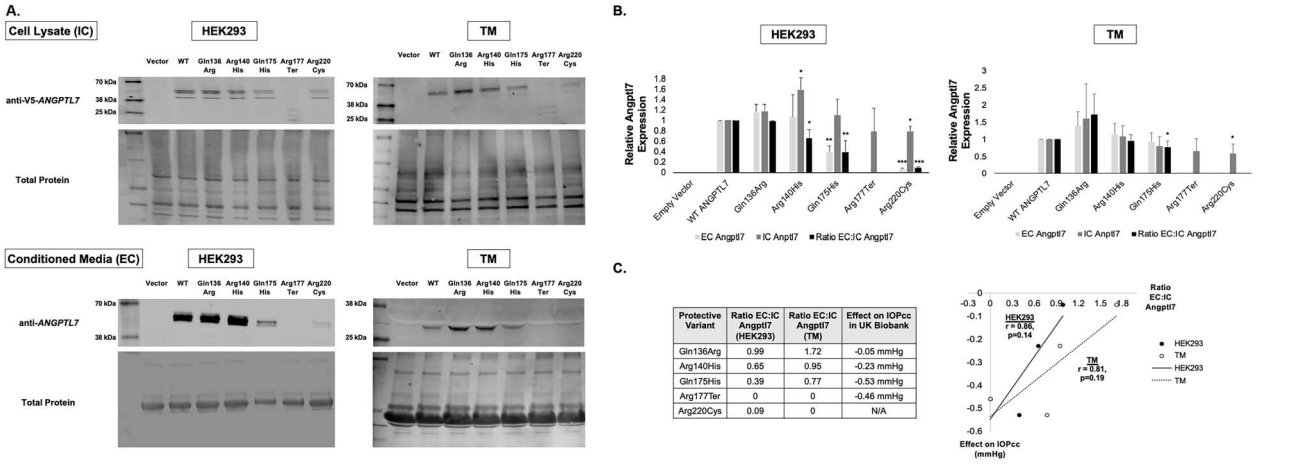

Figure 3. Intracellular (IC) and extracellular (EC) levels of wild-type (WT) and variant *ANGPTL7* protein in HEK293 and human TM cells. (**A**) Cells were transfected with an expression vector containing either empty vector, WT *ANGPTL7* or one of the five protective variants tagged with a V5-epitope. Each vector was tested in triplicate in HEK293 cells ($n = 3$); the findings were subsequently replicated in two TM strains from different donors, which were each tested in duplicate ($n = 4$). Whole-cell lysates and conditioned media were collected 48 hours post-transfection to measure IC and EC *ANGPTL7* levels, respectively. Anti-V5 antibody was used for the cell lysate samples since the V5 tag interfered with binding of anti-*ANGPTL7* antibody; given the V5 tag is cleaved prior to secretion, anti-*ANGPTL7* antibody was used for conditioned media samples. In both HEK293 and TM cells, western blot showed truncated IC protein products for the Arg177Ter nonsense variant, whereas all other variants showed protein products of expected size (~45 kDa with a doublet band due to post-translational glycosylation (10)). Of note, a smaller EC protein product was noted in TM cells compared with HEK293 cells, possibly due to proteolytic cleavage. There was no EC protein detected for the Arg177Ter and Arg220Cys variants in TM cells, whereas the other variants had variable levels of protein secretion. (**B**) EC, IC and the ratio of EC:IC protein levels was calculated for empty vector, WT *ANGPTL7* and each of the protective variants in both HEK293 and TM cells. The western blot band intensities were measured using ImageJ software. All data were normalized relative to total protein levels and subsequently normalized to wild-type *ANGPTL7*. Statistical analyses were performed using a one-way ANOVA (*$P < 0.05$, **$P < 0.01$, ***$P < 0.001$). (**C**) The correlation between the ratio of EC:IC *ANGPTL7* protein in TM cells and corneal-compensated intraocular pressure (IOPcc) lowering among individuals in the UK Biobank dataset (Table 1) was assessed using Pearson's correlation coefficient (r). Interestingly, there was a strong correlation between a lower EC:IC ratio and larger amounts of IOPcc lowering ($r = 0.86$ in HEK293 cells and 0.81 in TM cells), though this did not reach statistical significance due to a small number of data points ($P = 0.14$ in HEK293 cells and 0.19 in TM cells, $n = 4$ for each). These data suggest that the protective effect of *ANGPTL7* variants stems from lower amounts of secreted protein.

outflow pathway. Myocilin gene variants, for instance, are hypothesized to play a causal role in juvenile and primary open-angle glaucoma through a gain-of-function mechanism involving protein misfolding and chronic ER stress (13,14). Given that variant *ANGPTL7* proteins aggregate in the ER (Fig. 2), we tested whether these variants affect expression of ER stress markers.

HEK293 and primary cultures of human TM cells were transfected with either empty vector, WT *ANGPTL7* or one of the five protective variants tagged with a V5-epitope. Each vector was tested in triplicate in HEK293 cells ($n = 3$) and in duplicate in two different TM strains ($n = 4$). Whole-cell lysates were collected 48-hours post-transfection for western blot analysis. We tested expression of two different ER stress markers, Grp78 and Atf4, which are both elevated in Myocilin glaucoma and in other glaucoma models (14–16). Importantly, protective *ANGPTL7* variants did not affect expression of either Grp78 or Atf4 proteins relative to WT in either HEK293 or TM cells ($P > 0.05$ for all comparisons) (Fig. 4). Of note, different sized protein products were noted for Atf4 in TM cells compared with HEK293 cells; a variable Atf4 protein size between 40 and 50 kDa has been previously noted in different cell types (17,18).

Cyclic mechanical stress reduces *ANGPTL7* expression in the conventional aqueous outflow pathway

Elevated IOP is currently the only modifiable risk factor for POAG development and progression (19,20). *ANGPTL7* is highly expressed in the juxtacanalicular region (the site of greatest aqueous outflow resistance), suggesting that it plays a critical role in IOP regulation. (5,7)

Cells of the conventional outflow tract [TM and Schlemm's canal (SC) cells] reside in a mechanically demanding environment, as IOP fluctuates dynamically over the course of the day in both healthy and diseased eyes (21). These cells deform by up to 50% when IOP is elevated and return to their starting dimensions when IOP normalizes; giant vacuoles subsequently develop as pressure drops across the inner wall (22,23). To maintain homeostasis, TM and SC cells must adjust resistance and outflow facility, which is accomplished through cytokine release, alterations in target gene expression, increased ECM turnover and cytoskeletal reorganization (24,25).

We hypothesized that reduced expression of *ANGPTL7*, as seen with protective variants, are potentially a component of the homeostatic response to mechanical stress. To test this hypothesis, cultures of human TM and SC cells were subjected to 48 hours of CMS using the Flexcell strain unit (15% stretch at a frequency of 1 Hz, which mimics ocular pulse and is considered to be a physiologic level of CMS) (24–29). Control cells were plated on Flexcell plates but were not subjected to CMS. Three different TM and SC strains were tested, with each strain tested in triplicate ($n = 9$ for each). Data were normalized relative to *36b4* gene expression, as expression of this gene is not altered in response to CMS (30). qPCR demonstrated a significant reduction in *ANGPTL7* expression in SC cells after 48 hours of CMS (−2.4-fold-change, $P = 0.01$); a reduction was also noted in TM cells, though this did not reach statistical significance (−1.8-fold-change, $P = 0.21$) (Fig. 5). *PCDH10* (+25.9-fold-change, $P = 0.02$) and *IL6* (+5.9-fold-change, $P = 0.04$) served as positive controls for known cellular responses to CMS in TM and SC cells, respectively (30,31).

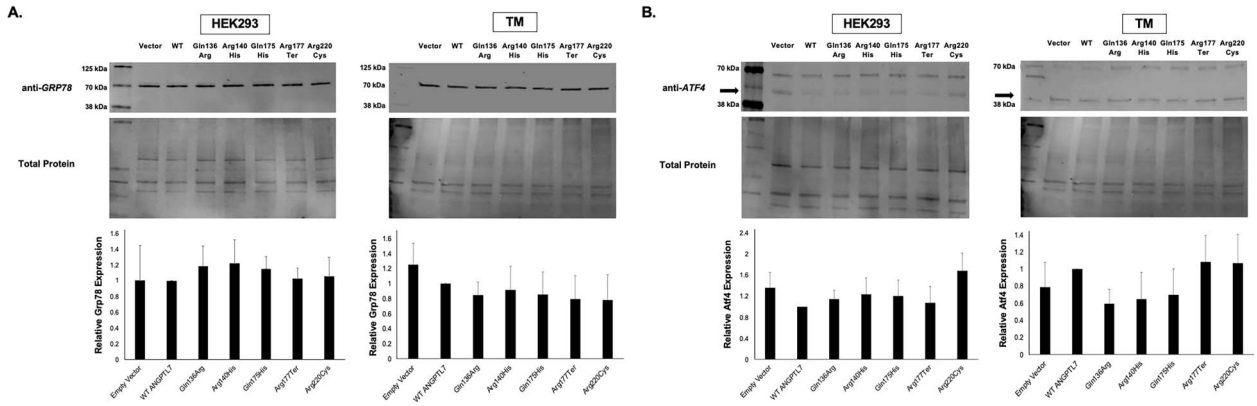

Figure 4. Protective *ANGPTL7* variants do not affect expression of endoplasmic reticulum (ER) stress markers in HEK293 and human TM cells**.** Cells were transfected with an expression vector containing either empty vector, WT *ANGPTL7* or one of the five protective variants tagged with a V5-epitope. Each vector was tested in triplicate in HEK293 cells ($n = 3$); the findings were subsequently replicated in two TM strains from different donors, which were each tested in duplicate ($n = 4$). Whole-cell lysates were collected 48 hours post-transfection to measure effects on expression of two different ER stress markers (Grp78 and Atf4). The western blot band intensities were measured using ImageJ software. All data were normalized relative to total protein levels and subsequently normalized to WT *ANGPTL7*; statistical analyses were performed using a one-way ANOVA. Protective variants did not affect expression of either of Grp78 or Atf4 relative to WT in either HEK293 or TM cells ($P > 0.05$ for all comparisons). Of note, different sized protein products were noted for Atf4 in TM cells compared with HEK293 cells (arrows); a variable Atf4 protein size between 40 and 50 kDa has been previously noted in different cell types (17,18).

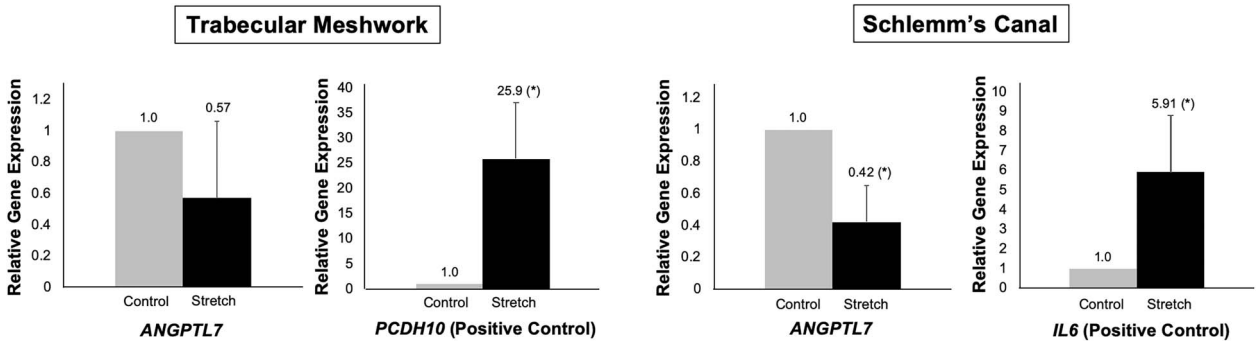

Figure 5. Cyclic mechanical stress (CMS) decreases *ANGPTL7* expression in the conventional aqueous outflow pathway**.** Primary cultures of human TM and Schlemm's canal (SC) cells were subjected to 48 hours of CMS using the Flexcell strain unit (15% stretch at a frequency of 1 Hz, which mimics ocular pulse and is considered to be a physiologic level of CMS (24–27,45)). Control cells were plated on Flexcell plates but were not subjected to CMS. Three different TM and SC strains were tested, with each strain tested in triplicate. Data were normalized relative to *36b4* gene expression, as expression of this gene is not altered in response to CMS. Statistical analyses were performed using a two-tailed *t*-test ($^*P < 0.05$). qPCR demonstrated a significant reduction in *ANGPTL7* expression in SC cells after 48 hours of CMS (−2.4-fold-change, $P = 0.01$); a reduction was also noted in TM cells, though this did not reach statistical significance (−1.8-fold-change, $P = 0.21$). *PCDH10* (+25.9-fold-change, $P = 0.02$) and *IL6* (+5.9-fold-change, $P = 0.04$) served as positive controls for known cellular responses to CMS in TM and SC cells, respectively (30,31).

Discussion

Over 120 genetic loci are strongly associated with risk for POAG (32,33). An important unmet need is the functional characterization of these gene variants to elucidate disease mechanisms, which will facilitate development of novel, targeted therapies. *ANGPTL7* is an attractive therapeutic target, as all known variants in this gene confer protection from POAG development. Moreover, this gene is highly expressed in the juxtacanalicular region of the aqueous outflow pathway and has altered expression in POAG patients compared with controls, providing evidence to support a functional role in disease pathogenesis (5–7).

In this study, we have characterized the five known missense and nonsense variants in the *ANGPTL7* gene, which were associated with lower IOP and reduced POAG risk in a rare variant analysis (3). We first used FoldX software to estimate protein stability for these variants compared with WT *ANGPTL7* protein. Interestingly, the protective variants with larger effect sizes had lower estimated protein stability. While it is critical to use caution when interpreting variant effect sizes, these data were nevertheless intriguing, as they suggested that the protective effects of *ANGPTL7* variants stem from reduced target protein levels. To experimentally support this hypothesis, we used western blot analyses to show that protective variants lead to reduced ratios of secreted:intracellular *ANGPTL7* protein relative to WT, which also correlates with variant effect sizes. Importantly, in contrast to Myocilin, accumulation of variant *ANGPTL7* protein does not increase ER stress. In addition to protective variants, we show that CMS also lowers *ANGPTL7* expression in the aqueous outflow pathway, suggesting that lower *ANGPTL7* levels are a component of the homeostatic response to dynamic IOP fluctuations.

The *ANGPTL7* gene was first hypothesized to play a causal role in glaucoma when microarray analyses demonstrated markedly increased expression in response to dexamethasone and TGF-β treatment in human TM cells (9,34). These *pathologic* cell stressors cause increased deposition of ECM material and reduced degradation, resulting in increased tissue stiffness and obstruction of aqueous outflow (35,36). In contrast, we investigated CMS, which

is a *physiologic* stressor that cells of the outflow tract continually encounter due to dynamic fluctuations in IOP. To respond to physiologic levels of mechanical stress, cells of the outflow tract, especially in the juxtacanalicular region, increase ECM turnover and degradation, which leads to increased outflow facility (37). In our CMS experiments, there was a significant reduction in *ANGPTL7* expression in SC cells, which directly interacts with the juxtacanalicular meshwork. While we also noted a reduction in *ANGPTL7* expression in TM cells, this did not reach statistical significance, likely due to the mix of trabecular beam cells and juxtacanalicular cells in the TM strains tested. The mix of trabecular beam cells and juxtacanalicular cells may also account for the lack of secreted *ANGPTL7* protein detected at baseline in the TM cell strains tested (Fig. 3A). In contrast, *ANGPTL7* protein was detected in all transfected samples, though with variable secreted:intracellular protein ratios among WT and variant proteins that were consistent in both HEK293 and TM cells. Replicating these findings at more physiologic levels of overexpression will be future experiments of interest.

It is important to note that outflow tissues in glaucomatous eyes have increased stiffness and display less movement in response to IOP fluctuations, potentially impacting the amount of mechanical stress they sense and respond to (38). Testing the effects of CMS on *ANGPTL7* expression in outflow cells from human donors with POAG will also be future experiments of interest.

Our work, along with prior studies, supports a model where *lower* levels of *ANGPTL7* mitigate pathologic accumulation of ECM material, while *higher* levels increase deposition. By reducing levels of *ANGPTL7* expression and secretion, rare protective variants may help maintain ECM homeostasis, leading to lower IOP and decreased risk for POAG.

Characterizing the impact of protective variants and relevant cell stressors in animal models will be an important next step. Additionally, it is important to determine whether aggregation of variant *ANGPTL7* protein stems from impaired protein folding and/or solubility. *ANGPTL7* may also interact with several ECM constituents to carry out its biological functions, including other glaucoma-associated proteins such as Myocilin and Efemp1; identifying these binding partners and assessing the impact of mutant protein aggregation on these binding interactions will improve understanding of disease mechanisms. Lastly, screening for inhibitors of *ANGPTL7* expression will pave the way for novel POAG therapies that target the genetic and molecular factors underlying disease development.

In summary, this is the first study, to our knowledge, to provide a possible functional mechanism whereby *ANGPTL7* gene variants confer protection from POAG. Further investigation of this mechanism may lay the groundwork for harnessing *ANGPTL7* downregulation as a novel preventative and therapeutic strategy for this common, blinding disease.

Materials and Methods

In silico protein stability calculations using FoldX

FoldX version 4.0 was used to estimate the effects of protective *ANGPTL7* variants on protein stability (11). The three-dimensional structure of WT *ANGPTL7* protein was downloaded as a PDB file from the AlphaFold database (39). The PDB structure was then repaired in the FoldX software to lower the global energy (ΔG). The target residues for each protective variant were then mutated individually and the difference in free energy ($\Delta\Delta G$) relative to WT *ANGPTL7* protein was calculated for each of the mutant proteins (a $\Delta\Delta G$ value $> +0.5$ indicates a destabilizing effect, while a value < -0.5 indicates a stabilizing effect; a value between -0.5 and $+0.5$ indicates a neutral change). Given the FoldX software does not enable analysis of nonsense mutations, the $\Delta\Delta G$ for the Arg177Ter mutation could not be calculated. The correlation between $\Delta\Delta G$ values and variant effects on IOPcc among individuals in the UK Biobank (3) was assessed using Pearson's correlation coefficient (r).

Cloning of *ANGPTL7* expression vectors

A gBlocks™ gene fragment containing WT *ANGPTL7* (NM_021146.4) and a 'CACC' directional sequence at the 5′ end was cloned into a pENTR™/D-TOPO™ entry vector per the manufacturer's protocol (ThermoFisher, Waltham, MA). Site-directed mutagenesis was performed using the QuikChange II kit (Agilent, Santa Clara, CA) for each of the protective variants individually (Table 1). The primers that were used for site-directed mutagenesis are listed in Supplementary Material, Table S1. The WT and mutant entry clones were then transferred to a Gateway destination expression vector modified to contain an N-terminal V5 epitope tag in-frame (pCAG-V5-IRES-EGFP) (12,40) using the LR Clonase™ II enzyme mix (ThermoFisher, Waltham, MA). Confirmatory sequencing was performed for all constructs.

Cell culture

Immortalized COS-7 (CRL-1651, ATCC, Manassas, VA) and HEK293 (CRL-1573, ATCC, Manassas, VA) cells were cultured in complete DMEM media (Gibco, Waltham, MA) supplemented with 10% FBS (Sigma, St. Louis, MO). Human TM and SC) endothelial cells were isolated from post-mortem non-glaucomatous donor eyes, cultured and characterized according to established protocols (41–43). These cells were cultured in complete DMEM media (Gibco, Waltham, MA) supplemented with 10% FBS (Sigma, St. Louis, MO) and 1% penicillin/streptomycin/glutamine (Gibco, Waltham, MA). All cells were grown at 37°C with 5% CO_2 and 85% humidity.

Immunohistochemistry

COS-7 cells and primary cultures of human TM cells were seeded on clear coverslips (Neuvitro, Vancouver, WA) in 12-well plates at a density of 100 000 cells/well. After ∼18 hours of growth, transfections were performed using Lipofectamine™ 3000 reagent (Invitrogen, Carlsbad, CA) according to the manufacturer's protocol. Transfections were performed using expression vectors containing WT *ANGPTL7* or one of the five rare protective variants (Table 1). Three independent transfections were performed for each vector in COS-7 cells ($n = 3$); the findings were then confirmed in two TM strains from different donors (ages 3 months and 54 years old), which were each tested in duplicate ($n = 4$). Immediately after transfection, CellLight™ ER-RFP BacMam 2.0 (Invitrogen, Carlbad, CA) was added to each well per the manufacturer's protocol to stain the ER.

The samples were processed for immunohistochemistry ∼24 hours post-transfection. After aspirating the conditioned media, the coverslips were washed with phosphate-buffered saline and fixed in 4% PFA. The samples were then permeabilized with 0.5% Triton X-100, blocked in 3% BSA, and incubated with a 1:1000 dilution of anti-V5-tag mouse monoclonal antibody overnight (ThermoFisher, Waltham, MA). The next day, the samples were incubated with a 1:1000 dilution of Alexa Fluor Plus 647 goat anti-mouse secondary antibody (Invitrogen, Carlsbad, CA) for 1 hour, followed by DAPI nuclear staining (ThermoFisher, Waltham, MA) for 1 minute. The coverslips were then mounted onto clear slides using ProLong™ Glass Antifade Mountant

(ThermoFisher, Waltham, MA) and imaged using the Leica SP8 confocal laser scanning microscope (Leica Microsystems, Wetzlar, Germany). For each slide, at least three images were taken at 20× magnification to assess the cellular localization pattern of WT *ANGPTL7* and each of the protective variants. Images of representative cells were then taken at 63× magnification with 2–5× zoom (Fig. 2).

Western blots

HEK293 cells and primary cultures of human TM cells were seeded in six-well plates at a density of 750 000 cells/well. After ∼18 hours of growth, transfections were performed using Lipofectamine™ 3000 reagent (Invitrogen, Carlsbad, CA) according to the manufacturer's protocol. Transfections were performed using either the empty expression vector, WT *ANGPTL7* or one of the five rare protective variants (Table 1). Three independent transfections were performed for each vector in HEK293 cells ($n = 3$); the findings were subsequently replicated in two TM strains from different donors (ages 3 months and 54 years old), which were each tested in duplicate ($n = 4$). Media was changed to serum-free DMEM ∼24 hours post-transfection.

The samples were processed for western blot ∼48 hours post-transfection. The conditioned media from each well was collected in cold Eppendorf tubes and centrifuged for 15 minutes at 4°C. The supernatant from each sample was then transferred to Amicon™ Ultra-0.5 centrifugal filter units (Sigma, St. Louis, MO) to concentrate the samples of conditioned media. To harvest whole-cell lysates, a mixture of cold RIPA buffer (Sigma, St. Louis, MO) and protease inhibitor (ThermoFisher, Waltham, MA) was added to each well and the plates were agitated for 30 minutes at 4°C. The samples were then transferred to cold Eppendorf tubes and centrifuged for 30 minutes at 4°C. The supernatant containing whole-cell lysates were collected and transferred to new Eppendorf tubes.

Protein concentrations for whole-cell lysate and conditioned media samples were measured using the Pierce™ BCA Protein Assay Kit (ThermoFisher, Waltham, MA) per the manufacturer's protocol. For each sample, 10 ug of protein was mixed with 4x Protein Sample Loading Buffer (Li-Cor, Lincoln, Nebraska), denatured by heating at 95°C for 5 minutes and loaded onto a 4%–20% Mini-PROTEAN® TGX™ Precast Protein Gel (Bio-Rad, Hercules, CA). Gel electrophoresis was performed at 120 V for ∼90 minutes. Proteins were then transferred from the gels onto polyvinylidene fluoride (PVDF) blotting membranes using the iBlot™ 2 system (Invitrogen, Carlsbad, CA).

The membranes were blocked for 1 hour using Intercept® blocking buffer (Li-Cor, Lincoln, Nebraska) and then incubated with a 1:1000 dilution of primary antibody overnight at 4°C. Antibodies tested included rabbit polyclonal anti-*ANGPTL7* (Proteintech, Rosemont, IL), mouse monoclonal anti-V5-tag (ThermoFisher, Waltham, MA), rat monoclonal anti-*GRP78* (Santa Cruz Biotechnology, Dallas, TX) and rabbit monoclonal anti-*ATF4* (Cell Signaling Technology, Danvers, MA). The next day, the membranes were washed and incubated with a 1:10 000 dilution of IRDye® 800CW secondary antibody (Li-Cor, Lincoln, Nebraska) for 1 hour (goat ant-rabbit, goat anti-mouse, or goat anti-rat, depending on the primary antibody used).

The membranes were then imaged on the 800-nm wavelength channel using the Odyssey CLx infrared imaging system (Li-Cor, Lincoln, Nebraska). To quantify total protein levels, the membranes were subsequently stained with the Revert™ 700 Total Protein Stain Kit (Li-Cor, Lincoln, Nebraska) per the manufacturer's protocol and imaged on the 700 nm wavelength channel using the Odyssey imaging system.

The density of western blot bands was measured using ImageJ software and normalized to total protein levels. All data were then normalized to WT *ANGPTL7* and statistically compared using a one-way ANOVA. A *P*-value <0.05 was defined as statistically significant. All statistical analyses were performed in STATA statistical software: release 16 (StataCorp LP, College Station, TX).

Cyclic mechanical stress in human TM and SC cells

Primary cultures of human TM and SC cells were seeded on six-well type I collagen-coated Flexcell plates (Flexcell, Burlington, NC) at a density of 100 000 cells/well. Cells were grown in DMEM supplemented with 10% FBS, which was switched to 1% FBS when cells reached ∼90% confluence (31,44). After 7 days, the medium was changed to serum-free DMEM and CMS was initiated ∼16 hours later. CMS was performed for 48 hours using a computer-controlled, vacuum-operated Flexcell FX-3000 Strain Unit (Flexcell, Burlington, NC). 15% stretch was performed at a frequency of 1 Hz, which mimics ocular pulse and is considered a physiologic level of CMS (24–27,45). Control plates were placed on the Flexcell apparatus but not subjected to CMS.

Three TM and three SC strains isolated from non-glaucomatous human donor eyes were tested, with each strain tested in triplicate. Donor ages were 35, 54 and 88 years for TM strains and 44, 59 and 77 years for SC strains. Samples were collected at the 48-hour timepoint and RNA was extracted from cells using the mirVana miRNA isolation kit (Ambion, Carlsbad, CA). cDNA was generated from RNA samples using the SuperScript™ IV VILO™ master mix (ThermoFisher, Waltham, MA) per the manufacturer's protocol.

Quantitative PCR

All qPCR experiments were performed on the QuantStudio™ 3 Real-Time PCR System (Applied Biosystems, Waltham, MA) using PowerTrack SYBR™ green master mix (ThermoFisher, Waltham, MA) per the manufacturer's protocol. Primers were designed to span exon-exon junctions and are listed in Supplementary Material, Table S1. Three technical replicates were performed for each reaction, which were averaged to obtain a mean Ct value. All data were normalized relative to 36b4 gene expression, as expression of this gene is not altered in response to CMS (30).

For the CMS experiments, control and stretch samples were statistically compared using a two-tailed *t*-test. A *P*-value <0.05 was defined as statistically significant. All statistical analyses were performed in STATA statistical software: release 16 (StataCorp LP, College Station, TX).

Supplementary Material

Supplementary Material is available at *HMG* online.

Conflict of Interest statement. W.D.S. is a member of the scientific advisory board for Broadwing Bio. J.L.W. has served as a consultant to Broadwing Bio, Allergan, Editas, Regenxbio and Aerpio. The authors have no other conflicts of interest to declare.

Funding

This work was supported by the National Institutes of Health/-National Eye Institute (R01 EY022305 to J.L.W., R01 EY030617 to W.D.S., P30 EY014104 to Massachusetts Eye and Ear, P30 EY005722

to Duke University) and Research to Prevent Blindness departmental grants to Massachusetts Eye and Ear and Duke University.

References

1. Quigley, H.A. and Broman, A.T. (2006) The number> of people with glaucoma worldwide in 2010 and 2020. *Br. J. Ophthalmol.*, **90**, 262–267.
2. Zhang, N., Wang, J., Li, Y. and Jiang, B. (2021) Prevalence of primary open angle glaucoma in the last 20 years: a meta-analysis and systematic review. *Sci. Rep.*, **11**, 13762.
3. Tanigawa, Y., Wainberg, M., Karjalainen, J., Kiiskinen, T., Venkataraman, G., Lemmela, S., Turunen, J.A., Graham, R.R., Havulinna, A.S., Perola, M. *et al.* (2020) Rare protein-altering variants in ANGPTL7 lower intraocular pressure and protect against glaucoma. *PLoS Genet.*, **16**, e1008682.
4. Santulli, G. (2014) Angiopoietin-like proteins: a comprehensive look. *Front. Endocrinol. (Lausanne)*, **5**, 4.
5. Patel, G., Fury, W., Yang, H., Gomez-Caraballo, M., Bai, Y., Yang, T., Adler, C., Wei, Y., Ni, M., Schmitt, H. *et al.* (2020) Molecular taxonomy of human ocular outflow tissues defined by single-cell transcriptomics. *Proc. Natl. Acad. Sci. USA*, **117**, 12856–12867.
6. Kuchtey, J., Kallberg, M.E., Gelatt, K.N., Rinkoski, T., Komaromy, A.M. and Kuchtey, R.W. (2008) Angiopoietin-like 7 secretion is induced by glaucoma stimuli and its concentration is elevated in glaucomatous aqueous humor. *Invest. Ophthalmol. Vis. Sci.*, **49**, 3438–3448.
7. van Zyl, T., Yan, W., McAdams, A., Peng, Y.R., Shekhar, K., Regev, A., Juric, D. and Sanes, J.R. (2020) Cell atlas of aqueous humor outflow pathways in eyes of humans and four model species provides insight into glaucoma pathogenesis. *Proc. Natl. Acad. Sci. USA*, **117**, 10339–10349.
8. Rozsa, F.W., Reed, D.M., Scott, K.M., Pawar, H., Moroi, S.E., Kijek, T.G., Krafchak, C.M., Othman, M.I., Vollrath, D., Elner, V.M. and Richards, J.E. (2006) Gene expression profile of human trabecular meshwork cells in response to long-term dexamethasone exposure. *Mol. Vis.*, **12**, 125–141.
9. Zhao, X., Ramsey, K.E., Stephan, D.A. and Russell, P. (2004) Gene and protein expression changes in human trabecular meshwork cells treated with transforming growth factor-beta. *Invest. Ophthalmol. Vis. Sci.*, **45**, 4023–4034.
10. Comes, N., Buie, L.K. and Borras, T. (2011) Evidence for a role of angiopoietin-like 7 (ANGPTL7) in extracellular matrix formation of the human trabecular meshwork: implications for glaucoma. *Genes Cells*, **16**, 243–259.
11. Schymkowitz, J., Borg, J., Stricher, F., Nys, R., Rousseau, F. and Serrano, L. (2005) The FoldX web server: an online force field. *Nucleic Acids Res.*, **33**, W382–W388.
12. Collantes, E.R.A., Delfin, M.S., Fan, B., Torregosa, J.M.R., Siguan-Bell, C., Vincent de Guzman Florcruz, N., Martinez, J.M.D., Joy Masna-Hidalgo, B., Guzman, V.P.T., Anotado-Flores, J.F. *et al.* (2022) EFEMP1 rare variants cause familial juvenile-onset open-angle glaucoma. *Hum. Mutat.*, **43**, 1343.
13. Jacobson, N., Andrews, M., Shepard, A.R., Nishimura, D., Searby, C., Fingert, J.H., Hageman, G., Mullins, R., Davidson, B.L., Kwon, Y.H. *et al.* (2001) Non-secretion of mutant proteins of the glaucoma gene myocilin in cultured trabecular meshwork cells and in aqueous humor. *Hum. Mol. Genet.*, **10**, 117–125.
14. Joe, M.K., Sohn, S., Hur, W., Moon, Y., Choi, Y.R. and Kee, C. (2003) Accumulation of mutant myocilins in ER leads to ER stress and potential cytotoxicity in human trabecular meshwork cells. *Biochem. Biophys. Res. Commun.*, **312**, 592–600.
15. Kasetti, R.B., Phan, T.N., Millar, J.C. and Zode, G.S. (2016) Expression of mutant myocilin induces abnormal intracellular accumulation of selected extracellular matrix proteins in the trabecular meshwork. *Invest. Ophthalmol. Vis. Sci.*, **57**, 6058–6069.
16. Peters, J.C., Bhattacharya, S., Clark, A.F. and Zode, G.S. (2015) Increased endoplasmic reticulum stress in human glaucomatous trabecular meshwork cells and tissues. *Invest. Ophthalmol. Vis. Sci.*, **56**, 3860–3868.
17. Ying, Y., Xue, R., Yang, Y., Zhang, S.X., Xiao, H., Zhu, H., Li, J., Chen, G., Ye, Y., Yu, M., Liu, X. and Zhong, Y. (2021) Activation of ATF4 triggers trabecular meshwork cell dysfunction and apoptosis in POAG. *Aging (Albany NY)*, **13**, 8628–8642.
18. Bezu, L., Sauvat, A., Humeau, J., Gomes-da-Silva, L.C., Iribarren, K., Forveille, S., Garcia, P., Zhao, L., Liu, P., Zitvogel, L. *et al.* (2018) eIF2α phosphorylation is pathognomonic for immunogenic cell death. *Cell Death Differ.*, **25**, 1375–1393.
19. Gordon, M.O., Beiser, J.A., Brandt, J.D., Heuer, D.K., Higginbotham, E.J., Johnson, C.A., Keltner, J.L., Miller, J.P., Parrish, R.K., 2nd, Wilson, M.R. *et al.* (2002) The Ocular Hypertension Treatment Study: baseline factors that predict the onset of primary open-angle glaucoma. *Arch. Ophthalmol.*, **120**, 714–720 discussion 829-730.
20. Heijl, A., Leske, M.C., Bengtsson, B., Hyman, L., Bengtsson, B., Hussein, M. and Early Manifest Glaucoma Trial, G. (2002) Reduction of intraocular pressure and glaucoma progression: results from the Early Manifest Glaucoma Trial. *Arch. Ophthalmol.*, **120**, 1268–1279.
21. Agnifili, L., Mastropasqua, R., Frezzotti, P., Fasanella, V., Motolese, I., Pedrotti, E., Di Iorio, A., Mattei, P.A., Motolese, E. and Mastropasqua, L. (2015) Circadian intraocular pressure patterns in healthy subjects, primary open angle and normal tension glaucoma patients with a contact lens sensor. *Acta Ophthalmol.*, **93**, e14–e21.
22. Grierson, I. and Lee, W.R. (1975) The fine structure of the trabecular meshwork at graded levels of intraocular pressure. (1) Pressure effects within the near-physiological range (8-30 mmHg). *Exp. Eye Res.*, **20**, 505–521.
23. Johnstone, M.A. (1979) Pressure-dependent changes in nuclei and the process origins of the endothelial cells lining Schlemm's canal. *Invest. Ophthalmol. Vis. Sci.*, **18**, 44–51.
24. Stamer, W.D. and Acott, T.S. (2012) Current understanding of conventional outflow dysfunction in glaucoma. *Curr. Opin. Ophthalmol.*, **23**, 135–143.
25. WuDunn, D. (2009) Mechanobiology of trabecular meshwork cells. *Exp. Eye Res.*, **88**, 718–723.
26. Acott, T.S., Vranka, J.A., Keller, K.E., Raghunathan, V. and Kelley, M.J. (2021) Normal and glaucomatous outflow regulation. *Prog. Retin. Eye Res.*, **82**, 100897.
27. Liton, P.B. and Gonzalez, P. (2008) Stress response of the trabecular meshwork. *J. Glaucoma*, **17**, 378–385.
28. Li, P., Shen, T.T., Johnstone, M. and Wang, R.K. (2013) Pulsatile motion of the trabecular meshwork in healthy human subjects quantified by phase-sensitive optical coherence tomography. *Biomed. Opt. Express*, **4**, 2051–2065.
29. Braakman, S.T., Pedrigi, R.M., Read, A.T., Smith, J.A., Stamer, W.D., Ethier, C.R. and Overby, D.R. (2014) Biomechanical strain as a trigger for pore formation in Schlemm's canal endothelial cells. *Exp. Eye Res.*, **127**, 224–235.
30. Youngblood, H., Cai, J., Drewry, M.D., Helwa, I., Hu, E., Liu, S., Yu, H., Mu, H., Hu, Y., Perkumas, K. *et al.* (2020) Expression of mRNAs, miRNAs, and lncRNAs in human trabecular meshwork cells upon mechanical stretch. *Invest. Ophthalmol. Vis. Sci.*, **61**, 2.

31. Hauser, M.A., Aboobakar, I.F., Liu, Y., Miura, S., Whigham, B.T., Challa, P., Wheeler, J., Williams, A., Santiago-Turla, C., Qin, X. *et al.* (2015) Genetic variants and cellular stressors associated with exfoliation syndrome modulate promoter activity of a lncRNA within the LOXL1 locus. *Hum. Mol. Genet.*, **24**, 6552–6563.
32. Gharahkhani, P., Jorgenson, E., Hysi, P., Khawaja, A.P., Pendergrass, S., Han, X., Ong, J.S., Hewitt, A.W., Segre, A.V., Rouhana, J.M. *et al.* (2021) Genome-wide meta-analysis identifies 127 open-angle glaucoma loci with consistent effect across ancestries. *Nat. Commun.*, **12**, 1258.
33. Aboobakar, I.F. and Wiggs, J.L. (2022) The genetics of glaucoma: disease associations, personalised risk assessment and therapeutic opportunities-a review. *Clin. Exp. Ophthalmol.*, **50**, 143–162.
34. Lo, W.R., Rowlette, L.L., Caballero, M., Yang, P., Hernandez, M.R. and Borras, T. (2003) Tissue differential microarray analysis of dexamethasone induction reveals potential mechanisms of steroid glaucoma. *Invest. Ophthalmol. Vis. Sci.*, **44**, 473–485.
35. Johnson, D., Gottanka, J., Flugel, C., Hoffmann, F., Futa, R. and Lutjen-Drecoll, E. (1997) Ultrastructural changes in the trabecular meshwork of human eyes treated with corticosteroids. *Arch. Ophthalmol.*, **115**, 375–383.
36. Wordinger, R.J., Sharma, T. and Clark, A.F. (2014) The role of TGF-beta2 and bone morphogenetic proteins in the trabecular meshwork and glaucoma. *J. Ocul. Pharmacol. Ther.*, **30**, 154–162.
37. Acott, T.S., Kelley, M.J., Keller, K.E., Vranka, J.A., Abu-Hassan, D.W., Li, X., Aga, M. and Bradley, J.M. (2014) Intraocular pressure homeostasis: maintaining balance in a high-pressure environment. *J. Ocul. Pharmacol. Ther.*, **30**, 94–101.
38. Gao, K., Song, S., Johnstone, M.A., Zhang, Q., Xu, J., Zhang, X., Wang, R.K. and Wen, J.C. (2020) Reduced pulsatile trabecular meshwork motion in eyes with primary open angle Glaucoma using phase-sensitive optical coherence tomography. *Invest. Ophthalmol. Vis. Sci.*, **61**, 21.
39. Tunyasuvunakool, K., Adler, J., Wu, Z., Green, T., Zielinski, M., Zidek, A., Bridgland, A., Cowie, A., Meyer, C., Laydon, A. *et al.* (2021) Highly accurate protein structure prediction for the human proteome. *Nature*, **596**, 590–596.
40. Zhang, Q., Liu, Q., Austin, C., Drummond, I. and Pierce, E.A. (2012) Knockdown of ttc26 disrupts ciliogenesis of the photoreceptor cells and the pronephros in zebrafish. *Mol. Biol. Cell*, **23**, 3069–3078.
41. Stamer, W.D., Seftor, R.E., Williams, S.K., Samaha, H.A. and Snyder, R.W. (1995) Isolation and culture of human trabecular meshwork cells by extracellular matrix digestion. *Curr. Eye Res.*, **14**, 611–617.
42. Stamer, W.D., Roberts, B.C., Howell, D.N. and Epstein, D.L. (1998) Isolation, culture, and characterization of endothelial cells from Schlemm's canal. *Invest. Ophthalmol. Vis. Sci.*, **39**, 1804–1812.
43. Keller, K.E., Bhattacharya, S.K., Borras, T., Brunner, T.M., Chansangpetch, S., Clark, A.F., Dismuke, W.M., Du, Y., Elliott, M.H., Ethier, C.R. *et al.* (2018) Consensus recommendations for trabecular meshwork cell isolation, characterization and culture. *Exp. Eye Res.*, **171**, 164–173.
44. Liton, P.B., Liu, X., Challa, P., Epstein, D.L. and Gonzalez, P. (2005) Induction of TGF-beta1 in the trabecular meshwork under cyclic mechanical stress. *J. Cell. Physiol.*, **205**, 364–371.
45. Johnstone, M.A. (2004) The aqueous outflow system as a mechanical pump: evidence from examination of tissue and aqueous movement in human and non-human primates. *J. Glaucoma*, **13**, 421–438.